




ARTICLE

A model-based approach leveraging in vitro data to support dose selection from the outset: A framework for bispecific antibodies in immuno-oncology

Javier Sánchez^{1,2}  | Christina Claus³ | Rosmarie Albrecht³ | Brenda C. Gaillard³ | Joana Marinho³ | Christine McIntyre⁴ | Tamara Tanos¹ | Axel Boehnke¹ | Lena E. Friberg²  | Siv Jönsson²  | Nicolas Frances¹

¹Roche Pharma Research and Early Development (pRED), Roche Innovation Center Basel, Basel, Switzerland

²Department of Pharmacy, Uppsala University, Uppsala, Sweden

³Roche Pharma Research and Early Development (pRED), Roche Innovation Center Zurich, Schlieren, Switzerland

⁴Roche Pharma Research and Early Development, Roche Innovation Center Welwyn, Welwyn Garden City, UK

Correspondence

Javier Sánchez, Roche Pharmaceutical Research and Early Development (pRED), Roche Innovation Center Basel, Grenzacherstrasse 124, 4070 Basel, Switzerland.
Email: javier.sanchez_fernandez@roche.com

Abstract

FAP-4-1BBL is a bispecific antibody exerting 4-1BB-associated T-cell activation only while simultaneously bound to the fibroblast activation protein (FAP) receptor, expressed on the surface of cancer-associated fibroblasts. The trimeric complex formed when FAP-4-1BBL is simultaneously bound to FAP and 4-1BB represents a promising mechanism to achieve tumor-specific 4-1BB stimulation. We integrated in vitro data with mathematical modeling to characterize the pharmacology of FAP-4-1BBL as a function of trimeric complex formation when combined with the T-cell engager cixutumumab. This relationship was used to prospectively predict a range of clinical doses where trimeric complex formation is expected to be at its maximum. Depending on the dosing schedule and FAP-4-1BBL plasma: tumor distribution, doses between 2 and 145 mg could lead to maximum trimeric complex formation in the clinic. Due to the expected variability in both pharmacokinetic and FAP expression in the patient population, we predict that detecting a clear dose–response relationship would remain difficult without a large number of patients per dose level, highlighting that mathematical modeling techniques based on in vitro data could aid dose selection.

Study Highlights

WHAT IS THE CURRENT KNOWLEDGE ON THE TOPIC?

FAP-4-1BBL is a tumor-specific 4-1BB costimulator. The clinical pharmacokinetics of FAP-4-1BBL, as well as some preclinical pharmacology, have been previously reported.

WHAT QUESTION DID THIS STUDY ADDRESS?

We developed a model-based workflow to integrate in vitro data to suggest a recommended dose-range to be explored in clinical trials.

This is an open access article under the terms of the [Creative Commons Attribution-NonCommercial-NoDerivs](https://creativecommons.org/licenses/by-nc-nd/4.0/) License, which permits use and distribution in any medium, provided the original work is properly cited, the use is non-commercial and no modifications or adaptations are made.

© 2023 The Authors. *CPT: Pharmacometrics & Systems Pharmacology* published by Wiley Periodicals LLC on behalf of American Society for Clinical Pharmacology and Therapeutics.

WHAT DOES THIS STUDY ADD TO OUR KNOWLEDGE?

We provide a range of doses worth exploring in the clinic. Moreover, our results suggest that observing a clear dose–response with molecules like FAP-4-1BBL in the clinic would require a large number of patients per dose level.

HOW MIGHT THIS CHANGE DRUG DISCOVERY, DEVELOPMENT, AND/OR THERAPEUTICS?

Traditional oncology drug development has relied on identifying the maximum tolerated dose. We show that this approach may not be required with molecules like FAP-4-1BBL. Additionally, we provide an in vitro data package and modeling workflow to support translational development of similar molecules.

INTRODUCTION

Cancer immunotherapy has revolutionized the treatment of multiple hematological and solid malignancies.^{1–3} Treatment with CD3 T-cell bispecific antibodies (TCBs) has the potential to redirect cytotoxic T-cells against tumor-specific antigens. Although TCBs are active in the preclinical setting,^{4,5} clinical monotherapy with TCBs in solid tumors has proven challenging.^{6,7} To this respect, combination of TCBs with other cancer immunotherapies have the potential to increase TCB effect and patient benefit.^{8,9}

In this work, we aim to optimize the combination of the TCB cibisatamab (RO6958688)^{4,10} with the bispecific fusion protein FAP-4-1BBL (RO7122290)^{9,11} by combining in vitro data with modeling and simulation. Preclinical experiments have shown an enhanced tumor cell killing and T-cell activation when combining cibisatamab and FAP-4-1BBL, both in vitro and in vivo.^{9,11} Cibisatamab binds to both the CD3 receptor on T-cells and the CEACAM5 receptor on tumor cells, whereas FAP-4-1BBL binds to both the fibroblast activation protein (FAP) on the surface of cancer-associated fibroblasts and the 4-1BB receptor on T-cell surface. [Figure 1a](#) illustrates the mechanism of action of cibisatamab and FAP-4-1BBL. As cibisatamab and FAP-4-1BBL do not pursue the same targets neither on T-cells nor in the tumor microenvironment, their binding kinetics are assumed independent. Here, we focus on optimizing therapy with FAP-4-1BBL; a similar work to understand the relationship between target engagement and T-cell activation with cibisatamab has already been published.¹² The formation of the trimeric complex versus bispecific concentration follows a bell-shaped curve¹³ as the trimeric complex formation increases with increasing concentrations up to a maximum, and further increase in bispecific concentration favors the formation of dimers (bispecific bound only to the T-cell or to the tumor-associated antigen). Assuming that trimeric complex formation ignites

enhanced T-cell mediated tumor cell killing, characterization of dose/exposure-trimeric complex relationship is important to support dose selection during early clinical development. To this regard, in vitro experiments allow testing a wide range of conditions (drug exposure, receptor expression levels in target and effector cells, antibody binding kinetics, etc.) in a well-controlled manner, thus providing a comprehensive characterization of the impact of such conditions in drug pharmacology. Mathematical models can then be used to integrate the available information, aiding in the translation between preclinical models and the clinical setting.

Costimulation via the 4-1BB (CD137) receptor of activated T-cells has been shown to increase the cytotoxicity and prevent the activation-induced cell death and exhaustion of the T-cells.^{14–16} However, attempts of stimulating the 4-1BB receptor with classical monoclonal antibodies have been hampered by toxicity and lack of clinical efficacy.^{17,18} Bispecific constructs targeting 4-1BB receptors on T-cells and a tumor-associated antigen^{9,11,19} exert T-cell activation only while forming a trimeric complex, and may serve as alternatives to avoid systemic T-cell activation while maximizing 4-1BB agonism in the tumor microenvironment. As FAP expression is restricted to the tumor-associated tissues, such as the tumor microenvironment and tumor draining lymph nodes (with other tissues expressing negligible levels of FAP),^{20,21} it represents a promising target to achieve tumor-specific 4-1BB stimulation with FAP-4-1BBL.

In this work, we combine in vitro data with mathematical modeling to characterize the pharmacological effect of FAP-4-1BBL as a function of trimeric complex formation when used in combination with cibisatamab. This relationship is thereafter used to prospectively predict the range of clinical doses where trimeric complex formation is expected to be at its maximum. In addition, we predict the impact of FAP expression (which differs from patient to patient in the population) in the projected increased tumor cell killing with cibisatamab

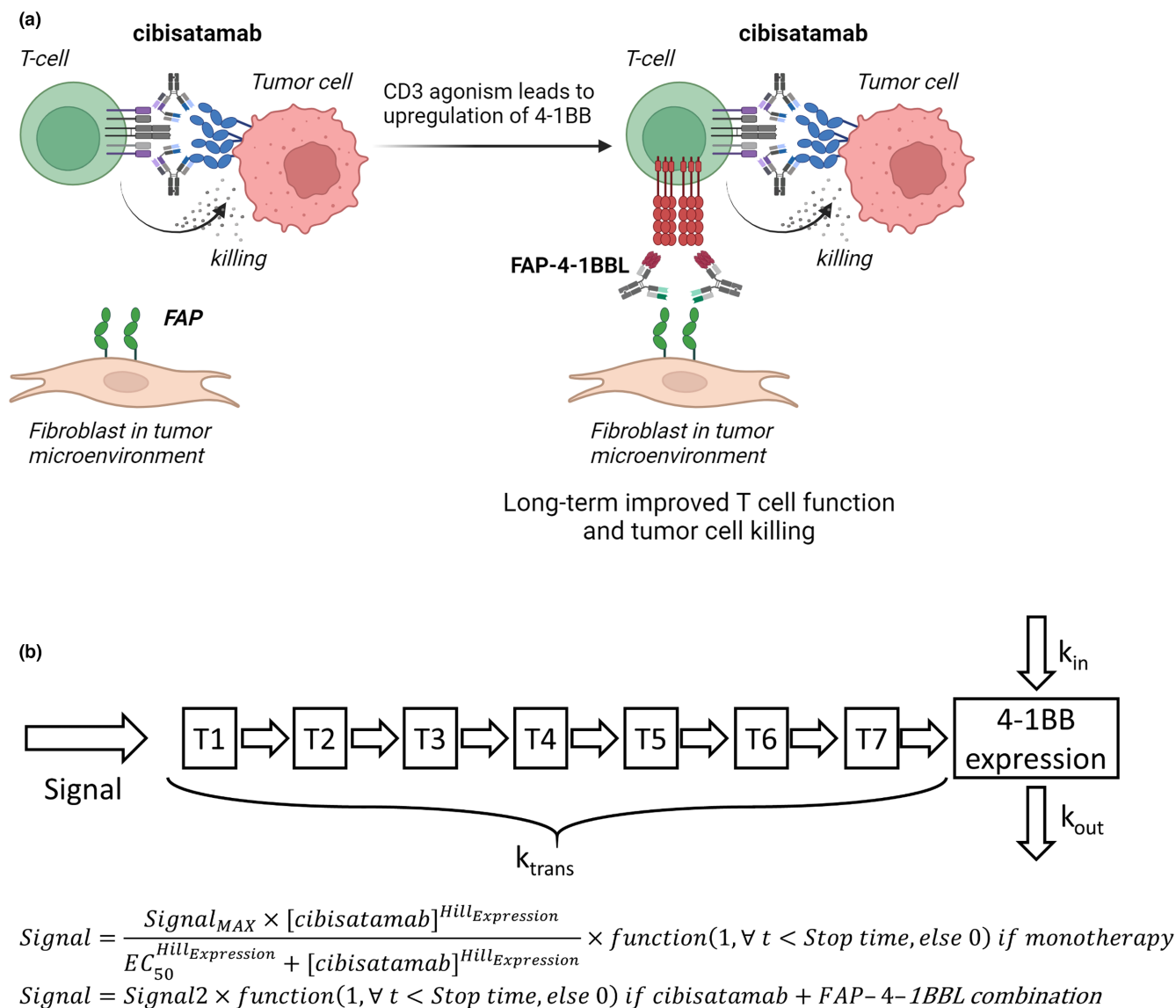


FIGURE 1 (a) Illustration of the mechanism of action of cibisatamab and FAP-4-1BBL. (b) Schematic representation of the structural model used to describe the time course of 4-1BB expression in the presence of cibisatamab ± FAP-4-1BBL. EC₅₀, half-maximal effective concentration.

combined with FAP-4-1BBL as compared to cibisatamab single-agent.

simulations were performed in R version 4.2.1²⁴ using the *rxode2* package.²⁵

MATERIALS AND METHODS

Computer software

The *minpack.lm* package²² was used for nonlinear least squares regression fitting (model 2 and model 3). Nonlinear mixed effects modeling was performed using Monolix version 2021R1.²³ Structural model selection was made based on goodness-of-fit plots, Akaike Information Criteria, and precision of parameter estimates. Model

In vitro experiments

Data from three different in vitro experiments were generated. Details about the experimental system setups are available in the Supplementary [Materials and Methods](#). In all experiments, 5000 MKN-45 tumor cells were used as target cells, with 5000 peripheral blood mononuclear cells as effector cells (effector: target ratio 1:1). Ten thousand fibroblasts were used to provide FAP expression.

Experiment 1: Evaluation of 4-1BB expression dynamics

Given that 4-1BB expression can be induced following treatment with a TCB, experiment 1 evaluated the changes in 4-1BB expression over time following continuous stimulation with cibisatamab (with or without FAP-4-1BBL) in the presence of tumor cells and FAP-expressing fibroblasts. This information was needed to simulate trimeric complex formation in further modeling steps. Concentrations of cibisatamab monotherapy at 0, 0.2, 2, 20, 200, and 2000 nM were tested, as well as 20 nM of cibisatamab combined with 1 nM of FAP-4-1BBL. The 4-1BB expression was evaluated at 4, 21, 45, and 69 h after the start of the stimulation.

Experiment 2: Impact of FAP-4-1BBL exposure and FAP expression in tumor cell killing with FAP-4-1BBL combined with cibisatamab

FAP-4-1BBL at 0, 0.01, 0.1, 1, 10, 100, 1000, and 10,000 nM was combined with 2 nM of cibisatamab in an in vitro system with fibroblasts expressing 12,700 FAP/fibroblast (low FAP expression), or 92,000 FAP/fibroblast (high FAP expression). This information was needed to establish the relationship between trimeric complex formation and in vitro tumor cell killing.

Experiment 3: Impact of different proportions of FAP-positive fibroblasts on the tumor cell killing of cibisatamab with or without FAP-4-1BBL

Cibisatamab at 0.2 nM with or without FAP-4-1BBL at 0.001, 0.025, 0.05, 0.075, 0.1, 1, or 10 nM was tested in an in vitro system with a total of 10,000 fibroblasts, of which 0%, 5%, 10%, 15%, 20%, 40%, 60%, or 100% expressed FAP, with the remaining fibroblasts not expressing FAP. This experiment quantitatively informed how increases in the proportion of FAP-positive fibroblasts affect tumor cell killing with cibisatamab with or without FAP-4-1BBL, given that FAP expression has been found to be immunosuppressive in the clinic.²⁶

Modeling and simulation

A modeling and simulation framework was developed utilizing the data from the preclinical experiments and a previously developed population pharmacokinetic (PK)

model in humans²⁶ (see [Table 1](#)). The framework comprised (i) a model describing the change in 4-1BB receptors per T-cell over time after cibisatamab ± FAP-4-1BBL, (ii) a model describing the decrease in tumor cell killing with cibisatamab monotherapy as a function of the proportion of FAP-positive fibroblasts in the cell culture system, and (iii) a model quantifying the tumor cell killing increase (with respect to cibisatamab monotherapy) due to FAP-4-1BBL trimeric complex formation when FAP-4-1BBL is combined with cibisatamab. Details about the model development are available in the Supplementary [Materials and Methods](#).

FAP-4-1BBL and cibisatamab clinical PK simulations

Clinical PK parameters using compartmental modeling were available for both FAP-4-1BBL²⁷ and cibisatamab ([Supplementary Materials](#)). FAP-4-1BBL PKs were described by a two-compartment model with parallel linear and nonlinear clearance, whereas cibisatamab PKs were described by a two-compartment model with linear clearance.

In the simulations, a 100 mg cibisatamab dose is administered over a 2 h infusion, followed by a 2 h infusion of FAP-4-1BBL at doses ranging from 1 to 180 mg. Simulations were performed for FAP-4-1BBL administration every week (q.w.), every 2 weeks (q2w) or every 3 weeks (q3w), with cibisatamab being administered every 3 weeks (q3w).

Two scenarios for FAP-4-1BBL plasma:tumor distribution were considered. In both, tumor distribution was assumed to follow first-order kinetics resulting in either a 2.2 or a 10:1 plasma: tumor-free concentration ratio (in range with published results²⁸). A summary of all the model parameters used in the clinical simulations is available in the Supplementary [Materials](#). Details about the simulation conditions and assumptions are available in the Supplementary [Materials and Methods](#).

RESULTS

Models

Model 1: Change in 4-1BB expression over time

The semimechanistic model illustrated in [Figure 1b](#) provided the best description of the time course of 4-1BB expression on T-cells, which increased with increasing cibisatamab concentrations and with addition of FAP-4-1BBL to cibisatamab. Parameter estimates are available in [Table 2](#). In the Supplementary [Materials](#), the Monolix

TABLE 1 Summary of developed models, conducted simulations, and their characteristics and/or conditions.

Model or simulation	Describes/evaluates	Data/model reference
Model 1	The endpoint used for modeling was the number of 4-1BB receptors per CD8+ T-cell. The change from baseline 4-1BB expression as a function of time, cibisatamab and FAP-4-1BBL concentration was described with a semimechanistic model.	Data from experiment 1
Model 2	The endpoint used for modeling was the area under the tumor cell killing versus time curve. A generalized logistic model quantified the decrease in tumor cell killing with cibisatamab single-agent as a function of the proportion of FAP-positive fibroblasts in cell culture system.	Experiment 3
Model 3	The endpoint used for modeling was the area under the tumor cell killing versus time curve. Predictions of number of trimeric complexes per T-cell are based on an integration of model 1 with the model described in. ¹⁵ An E_{\max} model quantifying the tumor cell killing increase with FAP-4-1BBL + cibisatamab versus cibisatamab alone as a function of trimeric complex formation with FAP-4-1BBL was developed.	Experiment 2 + model 1 + trimeric complex formation based on ref. 15
Simulation 1	Trimeric complex formation at different doses/dosing schedules in humans, considering IIV only in PK parameters and assuming a 2.2 or a 10 plasma:tumor ratio. Simulations were run for a total duration of 30 weeks. FAP-4-1BBL doses ranged from 1 to 180 mg for q.w., q2w, and q3w dosing regimens combined with 100 mg of cibisatamab q3w.	PopPK model ²⁴ + trimeric complex formation based on ref. 15
Simulation 2	Impact of FAP expression in clinical tumor cell killing, evaluated only during the first 120 h, assuming a 2.2 plasma: tumor ratio. FAP expression was extracted from the literature ²⁷ and incorporated in the model as explained in Supplementary Materials and Methods .	PopPK model, ²⁴ model 1, model 2, model 3
Simulation 3	Sample size to detect difference on tumor cell killing between doses, considering IIV both in PK parameters and FAP expression, assuming a 2.2 plasma:tumor ratio. Explored sample sizes ranged between three and 160 patients per dose level. Dose comparison was performed between the dose which maximizes trimeric complex formation, and doses 165-fold lower and 350-fold higher during the first week of treatment. Details on the methodology are available in the Supplementary Materials and Methods .	PopPK model, ²⁴ model 1, model 2, model 3

Abbreviations: E_{\max} , maximum effect; IIV, inter-individual variability; PK, pharmacokinetic; PopPK, population PK.

TABLE 2 Parameter estimates of Model 1.

Parameter	Description	Typical value (% RSE)	Standard deviation of the random effects (% RSE)
Signal _{MAX} (receptors/cell)	Maximum achievable signal value for cibisatamab	538 (12.9)	0.1 (FIX)
Cibisatamab _{50,Signal} (nM)	Cibisatamab concentration at which signal value is half of E_{\max}	16 (19.2)	0.1 (FIX)
Hill _{Expression}	Hill coefficient for signal as a function of cibisatamab concentration	0.210 (34.4)	0.1 (FIX)
Signal2 (receptors/cell)	Signal in cibisatamab 20 nM + FAP-4-1BBL 1 nM condition	382 (28.1)	0.1 (FIX)
Stop time (h)	Time after which signal value is 0	16.2 (18.9)	0.1 (FIX)
k_{trans} (h^{-1})	Transit rate constant	0.280 (5.2)	0.09 (31.7)
k_{in} (receptors/cell · h^{-1})	Basal 4-1BB synthesis rate	2.95 (21.5)	0.1 (FIX)
k_{out} (h^{-1})	4-1BB elimination rate constant	0.283 (19.0)	0.1 (FIX)
a (receptors/cell)	Additive component of the error model	5.36 (8.6)	—

Note: E_{\max} , maximum effect; RSE, relative standard error, where FIX denotes that the parameter was fixed during estimation.

code and model fits to each experimental condition (Figure S4) are available. Goodness-of-fit plots are available in the [Supplementary Materials and Methods](#), and demonstrated a good fit of the developed models to the experimental data (Figure S2).

A *Signal* triggered by cibisatamab monotherapy (*TCB*) or cibisatamab in combination with FAP-4-1BBL (*Signal2*) was assumed to drive 4-1BB expression. The signal triggered by cibisatamab monotherapy followed a sigmoid maximum effect (E_{\max}) relationship versus increasing cibisatamab concentrations (see Equation 3). The signal from the cibisatamab combination is a single value (*Signal2*), as only one combination condition (20 nM of cibisatamab + 1 nM of FAP-4-1BBL) was tested. The *Signal* variable (see Figure 1) was found to be short-lived following both cibisatamab monotherapy and its combination with FAP-4-1BBL, and was modeled to instantly decrease to zero after an estimated timepoint (*Stop time*). This *Stop time* parameter was found to be independent from both cibisatamab concentration and FAP-4-1BBL costimulation.

Then, seven transit compartments (T1–T7) best described (in terms of objective function value, residual unexplained variability, and precision of parameter estimates) the delay between administration of cibisatamab and peak in 4-1BB expression. The mean transit time was found to be 28.6 h.

The Equations 1–8 describe the changes in the numbers of 4-1BB receptors per T-cell with time as a function of cibisatamab concentration.

$$\text{Step function} = 0.5 \times (\tanh(10^{15} \times (\text{Stop}_{\text{time}} - \text{time})) + 1) \quad (1)$$

$$\text{Signal} = \frac{\text{Signal}_{\text{MAX}} \times [\text{cibisatamab}]^{\text{Hill}_{\text{Expression}}} \times \text{Step function}}{[\text{cibisatamab}]^{\text{Hill}_{\text{Expression}}} + \text{Cibisatamab}_{50, \text{Signal}}^{\text{Hill}_{\text{Expression}}}} \quad (2)$$

(*cibisatamab monotherapy*)

$$\text{Signal} = \text{Signal2} \times \text{Step function} \quad (3)$$

(*cibisatamab + FAP-4-1BBL comb.*)

$$k_{\text{in}} = k_{\text{in},0} \times \text{Step function} \quad (4)$$

$$\frac{d(T_1)}{dt} = k_{\text{trans}} \times (\text{Signal} - T_1) \quad (5)$$

$$\text{From } i = 2 \text{ to } i = 7: \frac{d(T_i)}{dt} = k_{\text{trans}} \times (T_{i-1} - T_i) \quad (6)$$

$$\frac{d(4\text{-}1\text{BB})}{dt} = k_{\text{trans}} \times T_7 - k_{\text{out}} \times 4\text{-}1\text{BB} + k_{\text{in}} \quad (7)$$

$$4\text{-}1\text{BB}_0 = \frac{k_{\text{in},0}}{k_{\text{out}}} \quad (8)$$

Model 2: Single-agent cibisatamab in vitro tumor cell killing decreases with increasing percentages of FAP-expressing fibroblasts in a co-culture system

Figure 2a illustrates that cibisatamab monotherapy tumor cell killing is at its maximum in absence of FAP-positive fibroblast in the co-culture system, and decreases with increasing proportions of FAP-positive fibroblasts. Such a decrease could arise from the immunosuppressive effect of FAP-positive fibroblasts,²⁶ and needed to be accounted for when aiming to optimize the combination of FAP-4-1BBL and cibisatamab. This behavior was captured in Equation 9. Final parameter estimates are presented in Table 3. Goodness-of-fit plots, demonstrating a good fit of the developed model to the experimental data, are available in the [Supplementary Materials and Methods](#) (Figure S2). Addition of FAP-4-1BBL to cibisatamab in this experiment also led to an increase in tumor cell killing which could be accounted for with the trimeric complex model (Figure S3).

$$\text{Tumor cell killing} = \text{Basal} - \left(\frac{\text{Maximum Decrease}}{1 + e^{-\text{Sigmoid Coefficient} \times (\text{Logit}(\% \text{ of FAP}) - \text{midpoint})}} \right) \quad (9)$$

Model 3: Effect of FAP expression and FAP-4-1BBL concentration on tumor cell killing

Trimeric complex formation with FAP-4-1BBL on T-cell surface was assumed to drive the increase in tumor cell killing when FAP-4-1BBL was combined with cibisatamab, as compared to cibisatamab monotherapy. A schematic representation of the target engagement considered in model 3 is shown in Figure 2b, together with goodness-of-fit plots (Figure S2). Equations 10 to 27 describe the trimeric complex formation process. The complete code to simulate trimeric complex formation in the clinic is available in the [Supplementary Material](#). The proportion of FAP-positive fibroblasts, as well as the number of FAP receptors per fibroblasts, are assumed to remain constant over time. The association constants of FAP-4-1BBL to 4-1BB are $k_{\text{on } 4\text{-}1\text{BB}}$ and $k_{\text{on } \text{FAP}}$, respectively. Binding of FAP-4-1BBL to the 4-1BB receptor or to the FAP receptor results in the formation of a FAP-4-1BBL-4-1BB dimer ($\text{Dimer}_{4\text{-}1\text{BB}}$) or FAP-4-1BBL-FAP dimer ($\text{Dimer}_{\text{FAP}}$), respectively. Both $\text{Dimer}_{\text{FAP}}$ and $\text{Dimer}_{4\text{-}1\text{BB}}$ can then bind to 4-1BB and FAP, respectively, resulting in the formation of a trimeric complex. Dissociation of both the trimeric complex and/or the

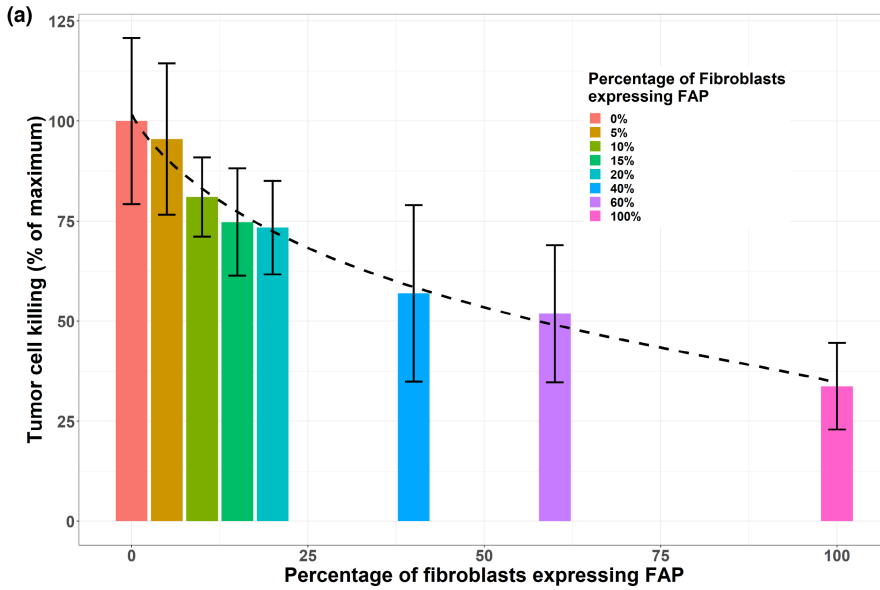
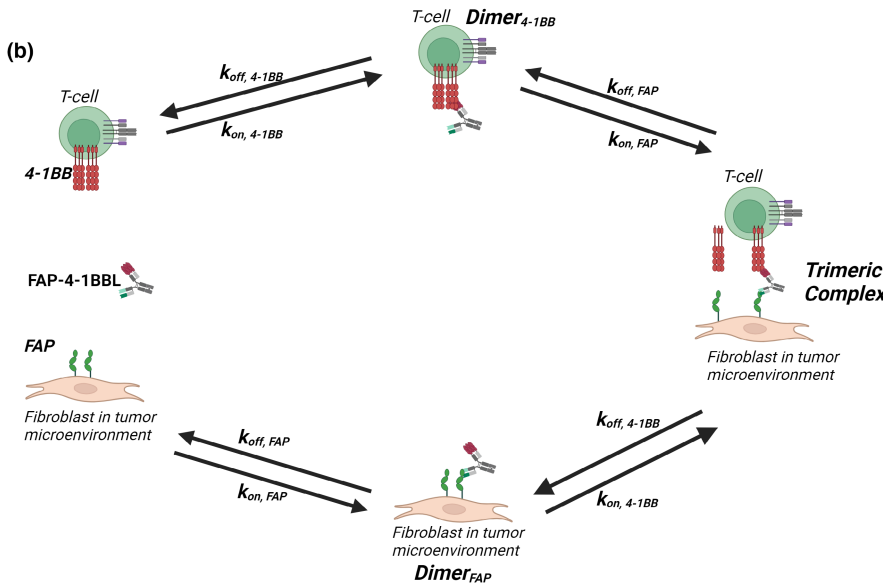


FIGURE 2 (a) Tumor cell killing normalized with respect to 0% of FAP-expressing fibroblast condition as a function of the percentage of fibroblasts expressing FAP in the in vitro system presented for experiment 3. Dashed line represents the model fitting to Equation 3. Error bars represent the mean \pm the standard deviation. (b) Schematic representation of the target engagement processes with FAP-4-1BBL included in model 3.



$Dimer_{FAP}$ and $Dimer_{4-1BB}$ species occur with rate constants $k_{off, FAP}$ and $k_{off, 4-1BB}$, respectively. The receptor occupancy (both for FAP and 4-1BB receptors) was defined as the percentage of receptors involved in formation of either Dimers or Trimeric complexes. The number of trimeric complexes on both FAP per fibroblast and 4-1BB per T-cell is defined as the percentage of receptors involved in trimeric complexes times the total number of receptors per cell.

$$\text{Step function} = 0.5 \times (\tanh(10^{15} \times (\text{Stop}_{time} - \text{time})) + 1) \quad (10)$$

$$\text{Signal} = \frac{\text{Signal}_{MAX} \times [\text{cibisatamab}]^{\text{Hill}_{Expression}} \times \text{Step function}}{[\text{cibisatamab}]^{\text{Hill}_{Expression}} + \text{Cibisatamab}_{50, \text{Signal}}^{\text{Hill}_{Expression}}} \quad (\text{cibisatamab monotherapy}) \quad (11)$$

$$\text{Signal} = \text{Signal2} \times \text{Step function} \quad (\text{cibisatamab} + \text{FAP-4-1BBL comb.}) \quad (12)$$

$$k_{in} = k_{in,0} \times \text{Step function} \quad (13)$$

$$\frac{d(T_1)}{dt} = k_{trans} \times (\text{Signal} - T_1) \quad (14)$$

$$\text{From } i = 2 \text{ to } i = 7: \frac{d(T_i)}{dt} = k_{trans} \times (T_{i-1} - T_i) \quad (15)$$

$$\begin{aligned} \frac{d(4-1BB)}{dt} = & k_{trans} \times T_7 - k_{out} \times 4-1BB + k_{in} - k_{on, 4-1BB} \\ & \times 4-1BB \times \text{FAP-4-1BBL} - k_{on, 4-1BB} \times Dimer_{FAP} \\ & \times 4-1BB + k_{off, 4-1BB} \times Dimer_{4-1BB} + k_{off, 4-1BB} \\ & \times \text{Trimeric} \end{aligned} \quad (16)$$

TABLE 3 Parameter estimates of model 2 and model 3.

Model	Parameter	Description	Estimate (% RSE)
Model 2 (decrease in tumor cell killing with cibisatamab single-agent as a function of the proportion of FAP-positive fibroblasts in cell culture system)	Basal _{No FAP+} (%)	Tumor cell killing with cibisatamab monotherapy in absence of FAP-positive fibroblasts	101.9 (3.6)
	Maximum decrease (%)	Maximum decrease in tumor cell killing with cibisatamab monotherapy due to FAP-positive fibroblasts	67.4 (7.8)
	Sigmoid _{Coefficient}	Hill coefficient of the sigmoid function	0.86 (16.8)
	Midpoint (logit of FAP-positive proportion)	Logit-transformation of FAP-positive fibroblast proportion at which 50% of the maximum decrease in tumor cell killing due to FAP-positive fibroblasts is achieved	−1.1 (21.3)
Model 3 (tumor cell killing increase with FAP-4-1BBL + cibisatamab versus cibisatamab alone as a function of trimeric complex formation with FAP-4-1BBL)	Killing _{MAX,combination}	Maximum fold increase in tumor cell killing with respect to cibisatamab monotherapy due to trimeric complex formation with FAP-4-1BBL	4.37 (3.7)
	Trimerics ₅₀	Number of trimeric complexes per T-cell at which fold increase in tumor cell killing is half of E_{max}	3.91×10^{-3} (16.5)
	Hill _{Kill,Combination}	Hill coefficient of fold increase in tumor cell killing as a function of trimeric complex formation	1.16 (17.4)
	Basal _{Killing,monotherapy}	Estimated tumor cell killing in absence of trimeric complex formation	1.04 (8.2)

Abbreviations: E_{max} , maximum effect; RSE, relative standard error.

$$\frac{d(\text{FAP})}{dt} = -k_{\text{on FAP}} \times \text{FAP} \times \text{FAP-4-1BBL} - k_{\text{on FAP}} \times \text{FAP} \times \text{Dimer}_{4-1\text{BB}} + k_{\text{off FAP}} \times \text{Dimer}_{\text{FAP}} + k_{\text{off FAP}} \times \text{FAP-4-1BBL} \quad (17)$$

$$\frac{d(\text{FAP-4-1BBL})}{dt} = -k_{\text{on FAP}} \times \text{FAP} \times \text{FAP-4-1BBL} - k_{\text{on 4-1BB}} \times 4-1\text{BB} \times \text{FAP-4-1BBL} + k_{\text{off FAP}} \times \text{Dimer}_{\text{FAP}} + k_{\text{off 4-1BB}} \times \text{Dimer}_{4-1\text{BB}} \quad (18)$$

$$\frac{d(\text{Dimer}_{\text{FAP}})}{dt} = k_{\text{on FAP}} \times \text{FAP} \times \text{FAP-4-1BBL} + k_{\text{off 4-1BB}} \times \text{Trimeric} - k_{\text{on 4-1BB}} \times \text{Dimer}_{\text{FAP}} \times 4-1\text{BB} - k_{\text{off FAP}} \times \text{Dimer}_{\text{FAP}} \quad (19)$$

$$\frac{d(\text{Dimer}_{4-1\text{BB}})}{dt} = k_{\text{on 4-1BB}} \times 4-1\text{BB} \times \text{FAP-4-1BBL} + k_{\text{off FAP}} \times \text{Trimeric} - k_{\text{off 4-1BB}} \times \text{Dimer}_{4-1\text{BB}} - k_{\text{on FAP}} \times \text{FAP} \times \text{Dimer}_{4-1\text{BB}} \quad (20)$$

$$\frac{d(\text{Trimeric})}{dt} = k_{\text{on 4-1BB}} \times \text{Dimer}_{\text{FAP}} \times 4-1\text{BB} + k_{\text{on FAP}} \times \text{FAP} \times \text{Dimer}_{4-1\text{BB}} - k_{\text{off FAP}} \times \text{Trimeric} - k_{\text{off 4-1BB}} \times \text{Trimeric} \quad (21)$$

$$\text{FAP}_0 = \text{Fibroblast}_{\text{number}} \times \frac{\text{FAP-positive fibroblasts}}{\text{Fibroblast}_{\text{number}}} \times \frac{\text{FAP receptors}}{\text{Fibroblast}} \times \frac{1 \text{ mol}}{N_{\text{Avogadro}}} \times \frac{10^9 \text{ nmol}}{1 \text{ mol}} \times \frac{1}{(\text{cell plate volume OR tumor volume})} \quad (22)$$

$$\text{Receptor Occupancy on FAP (\%)} = \frac{\text{Dimer}_{\text{FAP}} + \text{Trimeric}}{\text{FAP} + \text{Dimer}_{\text{FAP}} + \text{Trimeric}} \times 100 \quad (23)$$

$$\text{Receptor Occupancy on 4-1BB (\%)} = \frac{\text{Dimer}_{4-1\text{BB}} + \text{Trimeric}}{4-1\text{BB} + \text{Dimer}_{4-1\text{BB}} + \text{Trimeric}} \times 100 \quad (24)$$

$$\text{Trimerics on FAP per fibroblast} = \frac{\text{Trimeric}}{\text{FAP} + \text{Dimer}_{\text{FAP}} + \text{Trimeric}} \times \text{FAP receptor per fibroblast} \quad (25)$$

$$\begin{aligned} & \text{Trimerics on 4-1BB per T-cell} \\ &= \frac{\text{Trimeric}}{4\text{-1BB} + \text{Dimer}_{4\text{-1BB}} + \text{Trimeric}} \quad (26) \\ & \times 4\text{-1BB receptors per T-cell} \end{aligned}$$

Figure 3a displays the observed increased tumor cell killing resulting from the addition of FAP-4-1BBL to 2 nM of cibisatamab when the fibroblasts in the co-culture system express high and low levels of FAP. The bell-shaped tumor cell killing versus FAP-4-1BBL concentration is observed at both the low and high FAP expression conditions, with a maximum tumor cell killing close to 1 nM of FAP-4-1BBL.

Tumor cell killing was found to increase nonlinearly versus trimeric complex formation (Figure 3b; Equation 27). Table 3 presents the final model parameters, from which we derived that a maximum fold-increase in tumor cell killing in vitro of 4.4 relative to cibisatamab monotherapy can be achieved with the combination. To target a 90% of the maximum fold increase in tumor cell killing, 2.6×10^{-2} trimeric complexes per T-cell are needed.

$$\begin{aligned} \text{Fold increase} &= \left(\frac{\text{Killing}_{\text{EMAX,Combination}} - \text{Basal}_{\text{Killing,Monotherapy}}}{\text{Trimerics per T-cell}^{\text{Hill}_{\text{Kill,Combination}}}} \right) \\ & \times \frac{\text{Trimerics per T-cell}^{\text{Hill}_{\text{Kill,Combination}}} + \text{Trimerics}_{50}^{\text{Hill}_{\text{Kill,Combination}}}}{\text{Trimerics per T-cell}^{\text{Hill}_{\text{Kill,Combination}}} + \text{Trimerics}_{50}^{\text{Hill}_{\text{Kill,Combination}}} + \text{Basal}_{\text{Killing,Monotherapy}}} \quad (27) \end{aligned}$$

FAP per fibroblast required to achieve 90% of maximum fold increase in tumor cell killing with FAP-4-1BBL combined with cibisatamab versus cibisatamab monotherapy

Figure 3c shows the simulated average trimeric complex formed by FAP-4-1BBL per T-cells over 120 h versus FAP-4-1BBL concentration and FAP expression per fibroblast. From Figure 3c, it can be noted that an absolute minimum of 13,400 FAP per fibroblast (dashed black line) is required to form 2.6×10^{-2} trimeric complexes per T-cell and achieve 90% of the maximum tumor cell killing increase in combination with FAP-4-1BBL versus cibisatamab monotherapy. At this 13,400 FAP per fibroblast number, only a single FAP-4-1BBL concentration of 0.37 nM would lead to this 2.6×10^{-2} trimeric complexes per T-cell value. Conversely, FAP per fibroblast expressions higher than 13,400 FAP per fibroblast would allow the formation of at least 2.6×10^{-2} trimeric complexes per T-cell over a wide range of FAP-4-1BBL concentrations (e.g., with 100,000 FAP per fibroblasts, at least 2.6×10^{-2} trimeric complexes per T-cell can be achieved with FAP-4-1BBL concentrations between 0.01 to 11.5 nM). The area within the red line represents the conditions (in terms of FAP expression

and FAP-4-1BBL concentration) where at least 2.6×10^{-2} trimeric complexes per T-cell are formed.

Simulation 1: The doses which maximize trimeric complex formation for FAP-4-1BBL range between 3 mg and 21 mg, depending on dosing schedule

Figure 4 shows the area under the trimeric complex curve simulated for 30 weeks in the tumor at different doses and dosing schedules, with interindividual variability (IIV) being considered only for FAP-4-1BBL plasma PK. The dose leading to the greatest median area under the trimeric complex curve in the tumor ranged from 3 mg for a q.w. schedule assuming a 2.2 plasma: tumor ratio, to 67 mg for a q3w schedule assuming a 10 plasma: tumor ratio (during a 30-week treatment period, see Table 1 and FAP-4-1BBL Clinical Simulations in Supplementary Materials and Methods section). Doses between as low as 2 mg and as high as 145 mg would lead to less than a 20% drop from the maximum trimeric complex formation. Distribution of FAP-4-1BBL from plasma to tumor remains an uncertain parameter.

Simulation 2: FAP-positive tumor area evaluated by immunohistochemistry is not expected to be predictive of clinical outcome with FAP-4-1BBL + cibisatamab in a single-arm study

In Figure 5, we show the simulated trimeric complex formation in 1000 virtual patients with colorectal cancer (CRC) which differ in their FAP expression (see Simulation 2, Table 1), its associated increase in tumor cell killing versus cibisatamab monotherapy, and its associated absolute tumor cell killing (accounting for the decrease in cibisatamab tumor cell killing with the increase of FAP-positive fibroblasts in the tumor (see model 2 in Table 1). No further sources of IIV were considered for this analysis. From the figure, it can be noted that a greater percentage of FAP-positive fibroblasts in the tumor is expected to lead to greater trimeric complex formation, and greater fold increase in tumor cell killing versus cibisatamab monotherapy. This highlights that patients are expected to obtain some benefit from FAP-4-1BBL addition to cibisatamab. However, as cibisatamab tumor cell killing decreases with increasing proportions of FAP-positive fibroblasts (see model 2 in Table 1), in absence of comparative data with cibisatamab monotherapy, the percentage of FAP-positive fibroblasts in the tumor will not be predictive of the response to FAP-4-1BBL.

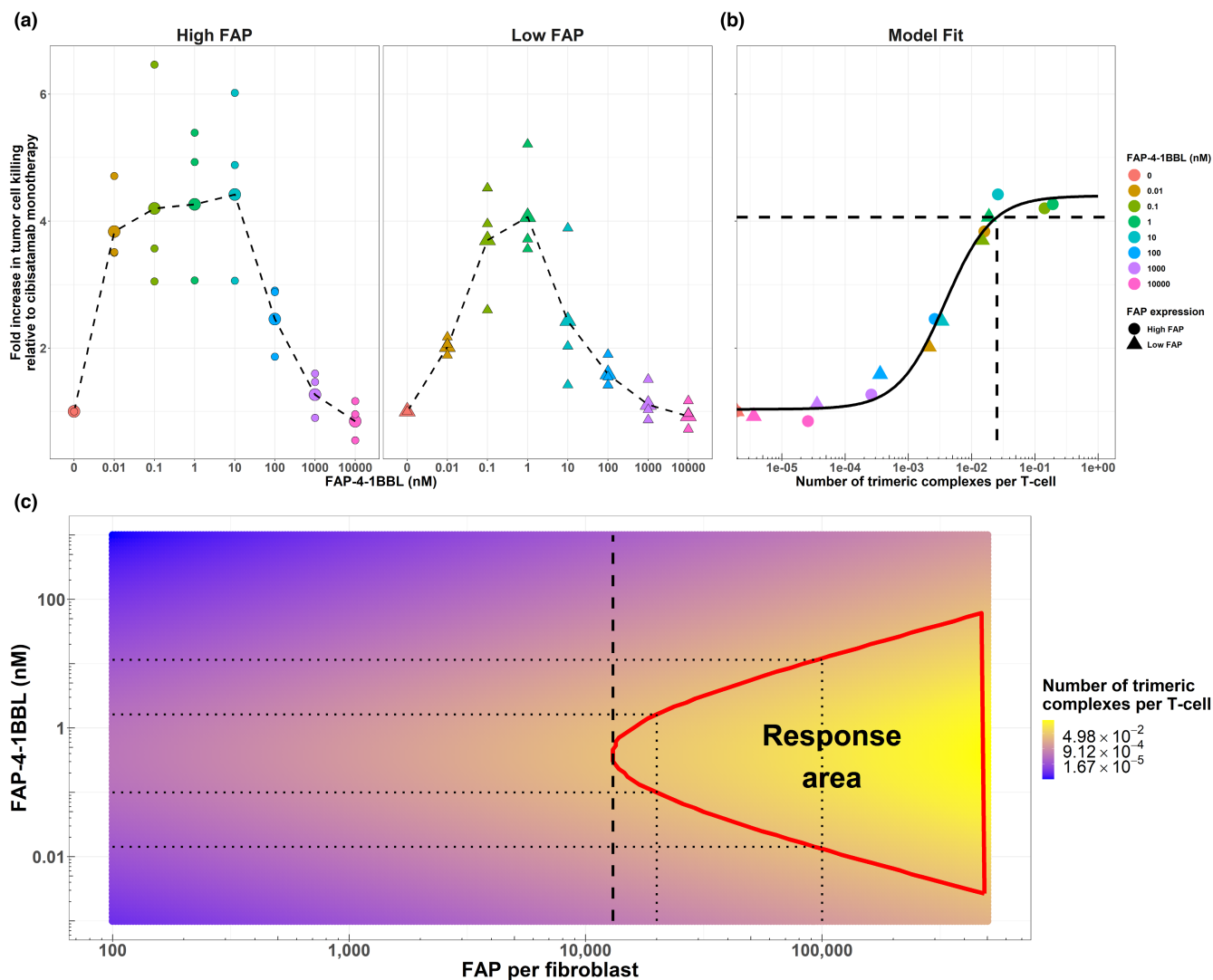


FIGURE 3 (a) Fold increase in tumor cell killing with respect to 2 nM cibisatamab monotherapy as a result of FAP-4-1BBL addition to a fibroblast co-culture in vitro system with high (left) and low (right) FAP expression levels. Large dots represent the mean of three technical replicates, with the small dots representing the value of each technical replicate. (b) Fold increase in tumor cell killing with respect to 2 nM cibisatamab monotherapy as a function of trimeric complex formation with FAP-4-1BBL on T-cells. Solid black line represents the fitting of Equation 26 to the data. Horizontal dashed line represents 90% of the maximum tumor cell killing increase as a result of trimeric complex formation with FAP-4-1BBL. Vertical dashed line represents the number of trimeric complexes per T-cell resulting in 90% of the maximum fold increase. (c) Dependency between FAP-4-1BBL concentration, number of FAP per fibroblast, and trimeric complex formation. Encircled area represents FAP expressions and FAP-4-1BBL concentrations with at least 2.6×10^{-2} trimeric complexes per T-cell and at least 90% of the maximum achievable fold increase in tumor cell killing with respect to cibisatamab monotherapy. Vertical dashed line represents the minimum 13,400 FAP/fibroblast needed to achieve this target trimeric complex formation.

Simulation 3: Number of patients per dose cohort to observe a significant difference in theoretical tumor cell killing

Figure 6 represents the number of patients needed to detect a statistically significant difference in tumor cell killing when comparing any dose to the dose which maximizes trimeric complex formation, at two different alpha (0.05 and 0.1) and beta (0.2 and 0.5) levels. The tumor cell killing was assumed to follow the same relationship versus trimeric complex and proportion of FAP-positive

fibroblasts as seen in vitro (see model 2 and model 3), with statistical significance determined by permutation test. The simulations are conducted assuming patient variability only from plasma PK and FAP expression (see Table 1), and a fixed plasma:tumor ratio of 2.2. The simulations are performed during the first week of treatment. Given that no other tumor or immune system characteristic which may influence pharmacology are considered, the number of patients needed to show a significant difference in terms of expected clinical tumor cell killing are underestimated. From this exercise, we observe that doses 0.35 to threefold

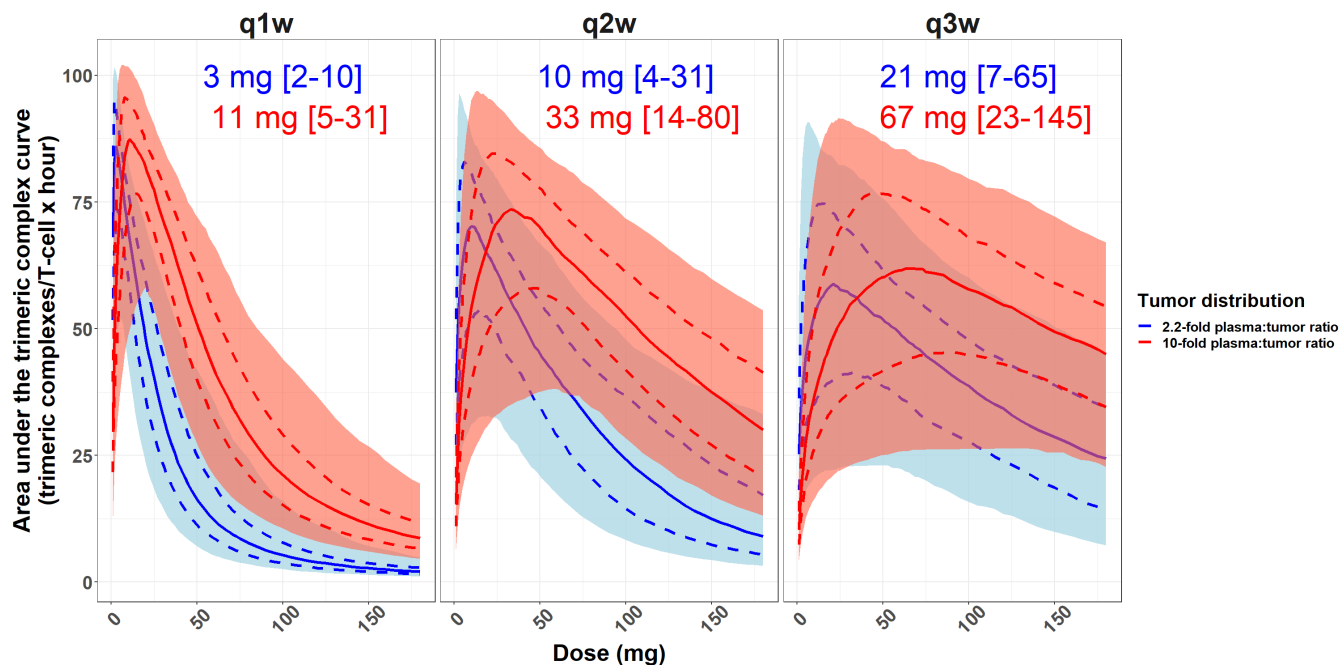


FIGURE 4 Area under the trimeric complex curve in the tumor at different doses, for different schedules (see Simulation 1, Table 1), at two different plasma:tumor distribution ratios. Solid lines represent the median of 1000 virtual patients, dashed lines represent the 25th–75th percentiles of 1000 virtual patients, and shaded areas represent the 5th–95th percentiles of 1000 virtual patients. Text annotations represent the dose at which trimeric complex formation is maximum and within brackets, the dose range at which trimeric complex formation drops no more than 20% from the maximum.

away from the dose that maximize trimeric complex formation could only be differentiated in a clinical trial with a high number of patients (more than 100 patients per dose group). Conversely, a statistically significant difference in tumor cell killing between the dose maximizing the trimeric complex formation and a dose 10-fold higher could be demonstrated in a clinical trial with about 35 patients per dose level. Under less stringent criteria (alpha level 0.1, 50% of power), a trend toward superiority can be detected with 15 patients per dose level when comparing the dose maximizing the trimeric complex formation and a dose about 10-fold higher.

DISCUSSION

In this study, we developed a PK/pharmacodynamic model integrating in vitro data to quantify the pharmacology of the tumor-targeted bispecific costimulator FAP-4-1BBL when used in combination with the CEACAM5-targeted T-cell bispecific cibisatamab.

We have shown by combining in vitro data with mathematical modeling that the FAP-4-1BBL pharmacological effect depends (solely based on preclinical data, not proven in clinic) on the number of trimeric complexes (molecular entities which comprise FAP-4-1BBL bound to the T-cell via 4-1BB and to cancer-associated fibroblasts

via FAP) formed on T-cells. We were able to quantitatively deconvolute the contribution of FAP-4-1BBL exposure, 4-1BB and FAP expressions on trimeric complex formation. Then, the number of trimeric complexes formed was associated to a pharmacological effect (tumor cell killing), and, assuming that these preclinical findings translate to the clinic, we predict that all patients would derive some benefit from the combination of cibisatamab with FAP-4-1BBL versus cibisatamab monotherapy, provided that enough FAP-4-1BBL trimeric complex is formed. Our in vitro data showed that a higher proportion of FAP-positive fibroblasts is associated with lower cibisatamab monotherapy activity, in agreement with the clinical findings of FAP-positive CRC tumors behaving more aggressively.²⁶ This information is incorporated in the model to better capture the associated effect in the cibisatamab plus FAP-4-1BBL combination simulations.

The model was developed based on in vitro data. We acknowledge that it may not reproduce all biological processes that play a role in the clinical response to the cibisatamab plus FAP-4-1BBL combination, such as the spatial distribution of FAP-expressing fibroblasts in the tumor, the different dynamics of de novo T-cell infiltration in the tumor, or the long-term changes in FAP expression on fibroblasts or 4-1BB expression on T cells. The range of clinical doses where we simulated the maximum trimeric complex formation in the tumor was derived by assuming

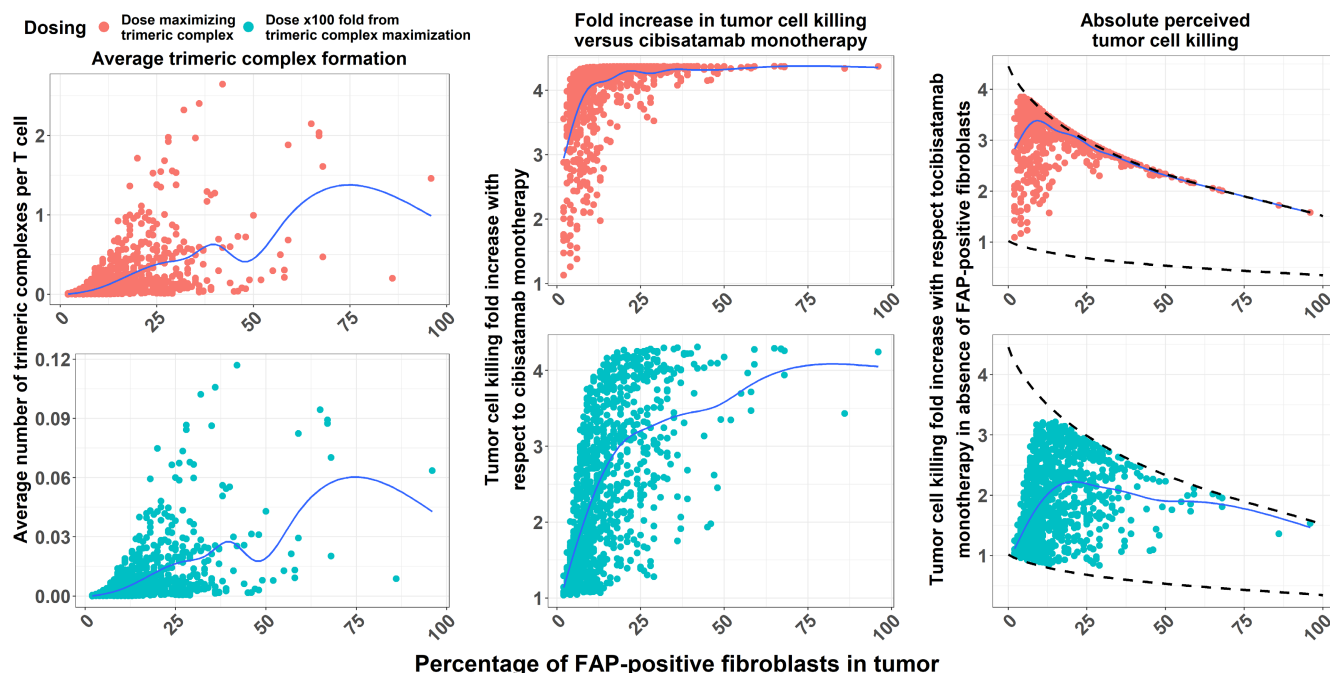


FIGURE 5 Average trimeric complex formation, associated fold increase in tumor cell killing with respect to cibisatamab monotherapy, and absolute tumor cell killing after considering decrease in cibisatamab monotherapy activity as a result of FAP-positive fibroblasts, for 1000 virtual patients treated with a dose maximizing trimeric complex or a dose 100-fold different from it. Blue solid lines represent a smoothed trendline, and black dashed lines represent the expected monotherapy effect (lower) and maximum possible combination effect (higher).

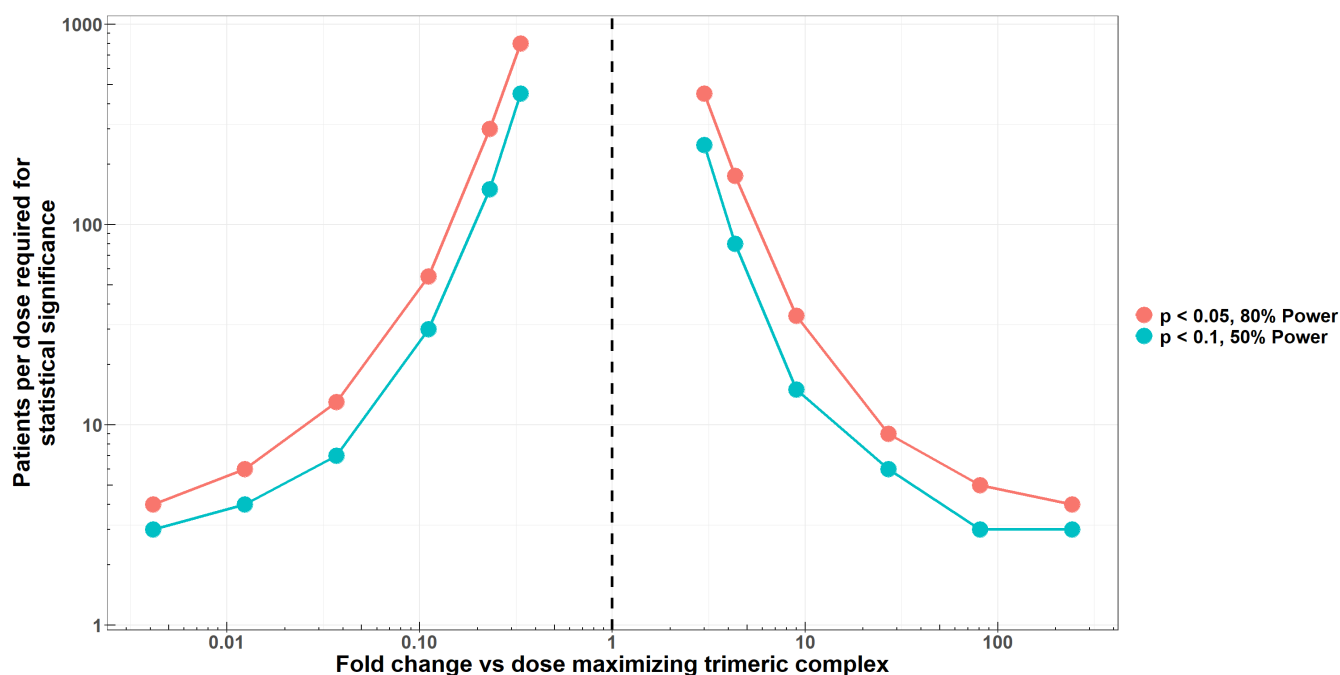


FIGURE 6 Number of patients per dose required to show a statistically significant difference in tumor cell killing between a given dose and the dose that maximizes the trimeric complex formation in the tumor. The vertical dashed line represents the dose maximizing trimeric complex formation in the tumor.

two different plasma:tumor partition coefficients of 2.2 and 10. In our model, FAP-4-1BBL tumor distribution remains a parameter with high uncertainty and high impact

in the range of clinical doses where we predict the maximum of trimeric complex formation. In addition, binding to soluble targets (both soluble FAP and/or soluble 4-1BB)

was not considered in this work, and could also impact trimeric complex formation in the tumor. Increases in soluble 4-1BB in serum have been observed in humans after administration of FAP-4-1BBL.¹⁶

The *in vitro* system used allows exploring the effect of cibisatamab plus FAP-4-1BBL combination only during a short period (up to 120 h after molecule addition). The combination demonstrated a marked benefit over cibisatamab alone in this time frame, but whether this benefit persists in the longer term requires further exploration. We focus on the added value of combining FAP-4-1BBL with cibisatamab, as compared to cibisatamab monotherapy. By doing so, we assume that cibisatamab monotherapy is active in all the patients. In reality, disease-control rate (percentage of partial responses plus percentage of stable diseases) with cibisatamab has been observed to occur in about 50% of the patients treated with cibisatamab single agent.⁷ Because of this, as we assume that all patients can derive benefit from the combination, the patient sample size we calculated to show a significant effect between two doses is likely underestimated.

Under the assumption of trimeric complex formation driving the benefit of FAP-4-1BBL combination with cibisatamab, we show how clinical dose-finding trials with bispecific costimulators (such as FAP-4-1BBL) should move away from the maximum tolerated dose paradigm, as recently cautioned by the Oncology Center of Excellence.²⁹ Instead, we propose exploring a range of clinical doses suggested from the integration of preclinical data using quantitative modeling.

With this work, we aim to provide recommendations for the early clinical development of bispecific costimulator antibodies based on the case example of FAP-4-1BBL in combination with cibisatamab. These recommendations can be expanded to other bispecific costimulators after specific adjustments based on the molecule format, target, or combination partner, and are presented below.

When it comes to clinical dose selection, our model simulations suggest that, due to variability in FAP expression, a comparison in outcome (tumor cell killing with FAP-4-1BBL combined with cibisatamab) between FAP-4-1BBL doses less than three-fold apart would require a high number of patients (more than 100 patients per dose level with our FAP-4-1BBL molecule example). These numbers were derived assuming that statistical significance is required in the dose comparison. Although Project Optimus specifically mentions that these trials need not be powered to detect statistically significant differences,³⁰ detecting a clear dose-response relationship would remain difficult without a large number of patients per dose level. The simulated dose range illustrates what could be a dose range explored in the clinic to explore the relationship between trimeric complex and response. It also illustrates

the challenges of establishing dose-response relationships with low numbers of patients per dose when comparing a narrow dose range. In this particular case, usage of preclinical data combined with modeling techniques could aid with dose selection. Conversely, our results suggest that a comparison between a dose maximizing trimeric complex formation in the tumor and doses about 14-fold higher with our FAP-4-1BBL molecule example would require less than 30 patients per dose level in our example.

With this work, we also aim to provide recommendations on a preclinical data package and modeling workflow to support clinical dose selection with similar molecules to FAP-4-1BBL. Specifically, *in vitro* systems allow testing a wide range of conditions, both in terms of bispecific costimulator concentrations and receptor expressions in target cells. A sufficiently wide range of bispecific costimulator concentrations should be tested preclinically to unravel the expected bell-shaped pharmacological effect versus exposure relationship. The associated trimeric complex bell shaped-curve can be derived from the binding properties of the antibody.¹³ The *in vitro* system bell shape exploration would provide, without mathematical modeling, the bispecific costimulator concentration leading to the maximum trimeric complex formation and pharmacological effect. This concentration can be compared to the measured free plasma concentrations from early clinical trials to facilitate clinical dose selection (factoring in the tumor distribution and its uncertainty).

Once a target exposure for the bispecific costimulator has been determined, it is important to understand under which conditions a patient will benefit the most from the treatment. In our case, we focused on both the 4-1BB and FAP expressions and their effect in pharmacology. We observed (from *in vitro* data) that a wide range of cibisatamab exposures would lead to marked 4-1BB expression. Concerning FAP expression and the expected benefit of the patient from the combination of cibisatamab with FAP-4-1BBL, we have shown that higher FAP expression leads to greater trimeric complex formation and greater benefit of FAP-4-1BBL addition to cibisatamab versus cibisatamab alone. However, because cibisatamab monotherapy effect decreases with greater proportions of FAP-positive fibroblasts in the tumor, the tumor percentage of FAP-positive fibroblasts in the clinic is not expected to predict the clinical benefit from the combination therapy. Nevertheless, it is important to note that all patients are expected to benefit more from the addition of FAP-4-1BBL to cibisatamab than from cibisatamab monotherapy, especially if FAP-4-1BBL exposures maximizing trimeric complex formation are achieved.

This work was done prospectively, before being able to determine an optimal dose with FAP-4-1BBL from clinical data. The developed model supported the clinical

development of FAP-4-1BBL, and is intended to be refined with further evidence from emerging clinical data, including biomarker data (plasma cytokine levels, soluble 4-1BB, and circulating immune cell counts) as well as tumor response data. The learnings can be implemented in other immunotherapy bispecific development programs.

CONCLUSIONS

FAP-4-1BBL in combination with cibisatamab increased in vitro tumor cell killing when compared to cibisatamab alone. The model quantified the increase in tumor cell killing as a function of the number of trimeric complexes on T-cells, which was then translated to the clinical setting to inform dose selection. The model suggests that, due to the expected PK and FAP expression variability, high (>100 patients per dose) sample sizes would be needed to detect a difference between doses as far as three-fold from the dose maximizing trimeric complex formation. As a result, we recommend incorporating modeling and simulation to inform dose ranges for clinical exploration.

AUTHOR CONTRIBUTIONS

J.S., L.E.F., S.J., and N.F. wrote manuscript. J.S., C.C., C.M., T.T., A.B., L.E.F., S.J., and N.F. designed the research. J.S., C.C., R.A., B.C.G., J.M., and N.F. performed the research. J.S. and C.C. analyzed the data. C.C., R.A., B.C.G., and J.M. contributed new reagents/analytical tools.

FUNDING INFORMATION

This study was funded by F. Hoffmann-La Roche Ltd.

CONFLICT OF INTEREST STATEMENT

J.S. and B.C.G. are employed by F. Hoffmann-La Roche Ltd. C.C., R.A., J.M., C.M., T.T., A.B., and N.F. are employed by F. Hoffmann-La Roche Ltd. and own Roche stock or stock options. L.E.F. works as an advisor for Pharmetheus AB, a company for pharmacometric services. S.J. is an employee at Pharmetheus AB, a company for pharmacometric services.

ORCID

Javier Sánchez  <https://orcid.org/0000-0002-8279-6916>
 Lena E. Friberg  <https://orcid.org/0000-0002-2979-679X>
 Siv Jönsson  <https://orcid.org/0000-0001-8240-0865>

REFERENCES

- Vaddepally RK, Kharel P, Pandey R, Garje R, Chandra AB. Review of indications of FDA-approved immune checkpoint inhibitors per NCCN guidelines with the level of evidence. *Cancers*. 2020;12(3):738.
- Kang C. Mosunetuzumab: first approval. *Drugs*. 2022;82(11):1229-1234.
- Kang C. Teclistamab: first approval. *Drugs*. 2022;82(16):1613-1619.
- Bacac M, Fauti T, Sam J, et al. A novel carcinoembryonic antigen T-cell bispecific antibody (CEA TCB) for the treatment of solid tumors. *Clin Cancer Res*. 2016;22(13):3286-3297.
- Nicolini VG, Waldhauer I, Freimoser-Grundschober A, et al. Abstract LB-389: combination of TYRP1-TCB, a novel T cell bispecific antibody for the treatment of melanoma, with immunomodulatory agents. *Cancer Res*. 2020;80(16 Supplement):LB-389.
- Harding JJ, Garrido-Laguna I, Chen X, et al. A phase 1 dose-escalation study of PF-06671008, a bispecific T-cell-engaging therapy targeting P-cadherin in patients with advanced solid tumors. *Front Immunol*. 2022;13:845417.
- Tabernero J, Melero I, Ros W, et al. Phase Ia and Ib studies of the novel carcinoembryonic antigen (CEA) T-cell bispecific (CEA CD3 TCB) antibody as a single agent and in combination with atezolizumab: preliminary efficacy and safety in patients with metastatic colorectal cancer (mCRC). *J Clin Oncol*. 2017;35(15_suppl):3002.
- Sam J, Colombetti S, Fauti T, et al. Combination of T-cell bispecific antibodies with PD-L1 checkpoint inhibition elicits superior anti-tumor activity. *Front Oncol*. 2020;10:575737.
- Claus C, Ferrara C, Xu W, et al. Tumor-targeted 4-1BB agonists for combination with T cell bispecific antibodies as off-the-shelf therapy. *Sci Transl Med*. 2019;11:eaa5989.
- Dudal S, Hinton H, Giusti AM, et al. Application of a MABEL approach for a T-cell-bispecific monoclonal antibody: CEA TCB. *J Immunother*. 2016;39:279-289.
- Trub M, Uhlenbrock F, Claus C, et al. Fibroblast activation protein-targeted-4-1BB ligand agonist amplifies effector functions of intratumoral T cells in human cancer. *J Immunother Cancer*. 2020;8(2):e000238.
- Van De Vyver AJ, Weinzierl T, Eigenmann MJ, et al. Predicting tumor killing and T-cell activation by T-cell bispecific antibodies as a function of target expression: combining in vitro experiments with systems modeling. *Mol Cancer Ther*. 2021;20(2):357-366.
- Betts A, van der Graaf PH. Mechanistic quantitative pharmacology strategies for the early clinical development of bispecific antibodies in oncology. *Clin Pharmacol Ther*. 2020;108(3):528-541.
- Palazon A, Teixeira A, Martinez-Forero I, et al. Agonist anti-CD137 mAb act on tumor endothelial cells to enhance recruitment of activated T lymphocytes. *Cancer Res*. 2011;71(3):801-811.
- Fisher TS, Kamperschroer C, Oliphant T, et al. Targeting of 4-1BB by monoclonal antibody PF-05082566 enhances T-cell function and promotes anti-tumor activity. *Cancer Immunol Immunother*. 2012;61(10):1721-1733.
- Melero I, Tanos T, Bustamante M, et al. A first-in-human study of the fibroblast activation protein-targeted, 4-1BB agonist RO7122290 in patients with advanced solid tumors. *Sci Transl Med*. 2023;15:eabp9229.
- Chester C, Sanmamed MF, Wang J, Melero I. Immunotherapy targeting 4-1BB: mechanistic rationale, clinical results, and future strategies. *Blood*. 2018;131(1):49-57.
- Segal NH, Logan TF, Hodi FS, et al. Results from an integrated safety analysis of Urelumab, an agonist anti-CD137 monoclonal antibody. *Clin Cancer Res*. 2017;23(8):1929-1936.

19. Muik A, Garralda E, Altintas I, et al. Preclinical characterization and phase I trial results of a bispecific antibody targeting PD-L1 and 4-1BB (GEN1046) in patients with advanced refractory solid tumors. *Cancer Discov.* 2022;12(5):1248-1265.
20. Juillerat-Jeanneret L, Tafelmeyer P, Golshayan D. Fibroblast activation protein- α in fibrogenic disorders and cancer: more than a prolyl-specific peptidase? *Expert Opin Ther Targets.* 2017;21(10):977-991.
21. Denton AE, Roberts EW, Linterman MA, Fearon DT. Fibroblastic reticular cells of the lymph node are required for retention of resting but not activated CD8+ T cells. *Proc Natl Acad Sci USA.* 2014;111(33):12139-12144.
22. Elzhov T, Mullen KM, Spiess A, Bolker B. minpack.lm: R Interface to the Levenberg-Marquardt Nonlinear Least-Squares Algorithm Found in MINPACK, Plus Support for Bounds. R package version 1.2-2 ed2022.
23. Monolix 2021R1, Lixoft SAS, a Simulations Plus company.
24. R Core Team. *R: A Language and Environment for Statistical Computing.* R Foundation for Statistical Computing; 2022.
25. Fidler M, Hallow M, Wilkins J, Wang W. RxODE: Facilities for Simulating from ODE-Based Models. R package version 2.0.13 ed2023.
26. Yang X, Lin Y, Shi Y, et al. FAP promotes immunosuppression by cancer-associated fibroblasts in the tumor microenvironment via STAT3-CCL2 signaling. *Cancer Res.* 2016;76(14):4124-4135.
27. Micallef S, Morcos PN, McIntyre C, et al. Using population pharmacokinetics to capture the binding of a novel bispecific fibroblast activation protein (FAP) to its 4-1BB ligand (4-1BBL) and support phase 2 dose selection in oncology patients. ACoP11; Virtual2020.
28. Eigenmann MJ, Karlsen TV, Wagner M, et al. Pharmacokinetics and pharmacodynamics of T-cell Bispecifics in the tumour interstitial fluid. *Pharmaceutics.* 2021;13(12):2105.
29. Shah M, Rahman A, Theoret M, Pazdur R. The drug-dosing conundrum in oncology—when less is more. *N Engl J Med.* 2021;385(16):1445-1447.
30. Oncology Center of Excellence (OCE), Food and Drug Administration. Draft guidance for industry: optimizing the dosage of human prescription drugs and biological products for the treatment of oncologic diseases. Guidance for Industry 2023.

SUPPORTING INFORMATION

Additional supporting information can be found online in the Supporting Information section at the end of this article.

How to cite this article: Sánchez J, Claus C, Albrecht R, et al. A model-based approach leveraging in vitro data to support dose selection from the outset: A framework for bispecific antibodies in immuno-oncology. *CPT Pharmacometrics Syst Pharmacol.* 2023;12:1804-1818. doi:[10.1002/psp4.13065](https://doi.org/10.1002/psp4.13065)